PHOTOIONIZATION STUDY OF THE CN-ANION:

A STUDY OF THE NaCN(001) SURFACE IN COMPARISON WITH CO AND N_2

by

H. Pulm, B. Marquardt and H.-J. Freund

Institut für Physikalische und Theoretische Chemie, Universität Erlangen-Nürnberg

R. Engelhardt

II. Institut für Experimentalphysik, Universität Hamburg

K. Seki, U. Karlsson and E.E. Koch

Hamburger Synchrotronstrahlungslabor HASYLAB at DESY

and

W. von Niessen

Institut für Physikalische und Theoretische Chemie
Technische Universität Braunschweig

Photoionization Study of the CN-Anion:

A Study of the NaCN(001) Surface in Comparison with CO and N_2 [*]

H. Pulm[+], B. Marquardt[+] and H.-J. Freund[++]

Institut für Physikalische und Theoretische Chemie
Universität Erlangen-Nürnberg
Egerlandstr. 3

D-8520 Erlangen, Fed. Rep. Germany

R. Engelhardt

II. Insitut für Experimentalphysik, Universität Hamburg
Luruper Chaussee 149

D-2000 Hamburg 50, Fed. Rep. Germany

K. Seki[o], U. Karlsson[oo] and E.E. Koch

Hamburger Synchrotronstrahlungslabor HASYLAB at DESY
Notkestr. 85

D-2000 Hamburg 52, Fed. Rep. Germany

and

W. von Niessen
Insitut für Physikalische und Theoretische Chemie
Technische Universität Braunschweig
Hans-Sommer Str. 10

D-3300 Braunschweig, Fed. Rep. Germany

Abstract

The results of a combined synchrotron uv-radiation and conventional XPS study on the (001)-surface of a NaCN single crystal are reported. Absolute valence and core binding energies of CN^- are deduced. The valence electron spectrum of NaCN is shown to be dominated by emission from the CN^- sublattice. Satellite structure is found in the inner valence electron region and consistently interpreted in comparison with CO and N_2. The experimentally determined electronic structure is compared with many-body ab-initio calculations of the ionization spectrum of CN^-. No band structure effects (k-dispersion) in the valence spectra are found due to the rotational disorder of the CN-sublattice. The branching ratios of the outer valence levels are determined, and shape resonances in both σ-levels are observed. The energies of the shape resonances in CN^- are compared with gaseous, condensed and adsorbed CO and N_2.

[+] Present address: Lehrstuhl für Theoretische Chemie, Universität zu Köln
Greinstr. 4, D-5000 Köln 41, Fed. Rep. Germany

[++] Author to whom correspondence should be addressed

[o] Permanent address: Institute for Molecular Science, Myodaiji, Okazaki 444
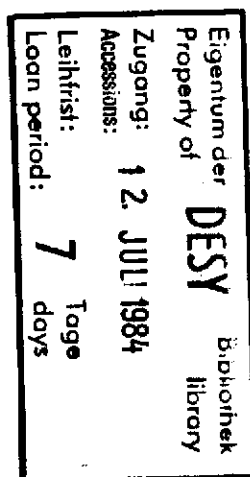Japan

[oo] Permanent address: Department of Physics, Linköping University,
S-58183 Linköping, Sweden

Introduction

In recent years progress has been made to understand the photoionization of diatomic molecules, such as CO and N_2, in the gas phase[1], the condensed solid phase[2] and in adsorbate phases[1].

Of particular interest has been the energy dependence of the photoionization cross section due to the observation of molecular shape resonances[3]. It has been shown recently, that energetic position and intensity of such shape resonances are considerably influenced by binding the free molecule to a metal surface[1,4]. This is probably due to the change of the potential felt by the escaping electron caused by a redistribution of the electron density upon binding a molecule to the surface. Also, scattering from the surface could effect such resonances.

Another point of current interest, that has attracted the attention of both theoreticians[5] and experimentalists[6,7], is the explanation of satellite structure found in the inner valence electron region. Very recently, the energy dependence of the intensity of these satellites in N_2 and CO have been studied in the gas and condensed phases.[6,7]

In this study we want to investigate the photoionization of $CN^{\ominus}$. We have chosen this system for two reasons:

i) $CN^{\ominus}$ is isoelectronic with CO and N_2.

ii) The electron distribution in $CN^{\ominus}$ is different from CO and N_2[8-12].

The photoionization of $CN^{\ominus}$ therefore allows us to investigate the influence of the altered charge distribution on position and intensity of the photoemission bands including the satellite structure in the inner valence region. Furthermore it serves as a model to study the influence of the altered wavefunction on the position of the shape resonance. The results can be compared with free condensed and adsorbed CO and N_2.

Since CN^- is an anion its study in the gas phase is hampered. CN^-, however, forms stable alkalicyanide crystals with rock salt structure at room temperature as shown in fig. 1a[13,14]. Due to the large electron affinity (3.82 eV[15]) of CN^-, which is even larger than that of fluorine, the rock salt lattice points of NaCN, for example, are occupied by Na cations and the barry centers of the CN^- anions, respectively. An oriented CN moiety would not allow for the high cubic symmetry of a rock salt crystal. The cubic symmetry originates from the rotational mobility of the CN units[14,16]. The rotational distribution, however, is not isotropic as shown in fig. 1b, which has been taken from the neutron diffraction work of Rowe et al.[16]. To a certain degree we can therefore look at an NaCN crystal at room temperature as a condensed coulomb stabelized CN^- gas, where the intermolecular separation between the CN^- moieties is approximately 4.2 Å .

By pressure and temperature variation NaCN and other alkalicyanides undergo several phase transitions. At a transition temperature of 288 K the rotational freedom of the CN^- anions is frozen along the (110)-direction[17] and the mechanical properties change rather dramatically. Resently, there is a wide interest in alkalicyanides from this point of view.[18]

Using angle resolved photoemssion with synchrotron radiation and angle integrated x-ray photoelectron spectroscopy we investigate the complete outer and inner valence electron region as well as the CN^- core ionizations of a (100) surface of a NaCN single crystal in normal emission. By comparison with solid and gaseous CO and N_2 relative binding energy differences and branching ratios intermediate between CO and N_2 are found. We observe satellite structure in the inner valence electron region and present an assignment analogous to CO and N_2[7] in comparison with many - body ab-initio calculations. It is found that the relative ionization potential of the CN-σ-bond is lowered with

respect to the lone pairs in comparison with CO and N_2 by approximately 3 eV which is in line with theoretical predictions based on one-particle properties.

The determined branching ratios of the three ion states lowest in energy in normal emission are compared with CO and N_2 and angle integrated measurements using unpolarized resonance lamp radiation[20]. The comparison indicates that we oberve the influence of the anisotropic orientation of the CN^- moieties. The branching ratios determined in normal emission show shape resonance structures that are shifted in energy relative to those of CO and N_2.

The paper is organized as follows: First we review the experimental procedures. The second part briefly summarizes the calculational details. In the third part we discuss the experimental results and compare them with results in the literature and our own theoretical considerations. Also, a brief excurs to adsorbates is presented. The fifth and last part contains a synopsis.

Experimental Procedure

The synchrotron experiments were performed at the storage ring DORIS in Hamburg. The synchrotron light was dispersed by a 1m-Seya-Namioka-Monochromator with concave gratings. The photon flux was monitored with a photodiode during the measurements. We recorded the electron distribution curves with a modified VG(ADES 400)-System in normal emission with an angular resolution of $\pm 1^o$. The overall resolution was $\Delta E = 0.25$ eV for $h\nu < 40$ eV, $\Delta E = 0.4$ eV for $h\nu = 40$ eV and $\Delta E = 0.55$ eV for $h\nu = 45$ eV. A detailed description of the experimental set up can be found in ref.[21]. Photoemission experiments using a conventional x-ray source with Mg- and Si- anodes were performed in a separate system using a modified Leybold-Heraeus (LHS 10) spectrometer[22]. The sample was a highly purified NaCN single crystal which was cleaved "in vacuo" along the {100} direction within a preparation chamber. After cleavage the sample was transfered under UHV into the measuring position. In order to fix the crystal onto the sample holder it was pressed into metallic indium. The pressure in the system was kept in the 10^{-10} Torr range.

Typical photoelectron distribution curves from the NaCN crystal are shown in fig. 2. They have been measured at room temperature. The zero of the intensity scale refers to the spectrum at the bottom. The energy scale was fixed with respect to the reported values of metallic indium[23].

For evaluating the branching ratios $B^1 = A_i / \sum_i A_i$ where A_i is the emission intensity of the i-th state and the sum is over all observed states of the ion the data were further processed. For the determination of photoemission intensities the electron distribution curves for each excitation energy were normalized to the intensity of the photon flux impinging onto the sample.

Furthermore a smooth structureless background was subtracted to account for
scattered secondary electrons. Finally,the area under each emission peak
in the electron distribution curves was determined by fitting the experimen-
tally observed three peak structure by three Gaussians corresponding to the
three uppermost ion states. The branching ratios are plotted in fig. 3 as
a function of photon energy.

Computational Procedures

Standard LCAO-MO-SCF calculations were carried out for CO,N_2 and CN^- using
the ORBIT-84 -program[24] , specifically designed for ab-initio calculations
on a simple micro computer. All integrals were calculated analytically over
carthesian gaussian type functions[25,26]. Two basis sets, i.e. a minimal
basis, STO 3G [27], and a split valence basis, 3-21G[28] , were employed.
No further optimization was tried for the 3-21G basis set. For the STO-3G
basis set the π-orbital exponents were slightly altered, due to their strong
influence on orbital and total energies. There are reports of better calculations
in the literature[10], but they are not directly comparable for the three
systems . All calculations were carried out using experimental geometries. The
results for the three systems with 3-21G basis are collected in table 1.

In addition to these calculations Green´s function computations have
been performed on the CN anion at an intermolecular separation of 0.118 nm.
The Green´s function calculations are based on ab-initio SCF calculations
and include the effects of electronic correlation and reorganization. Two
types of appoximations in the framework of the Green´s function method have
been employed. The first method is based on a finite perturbation expansion
of the self energy. All terms up to and including the third order terms
in the electron-electron interaction are taken into account. Higher order
terms are approximated by a renormalization procedure. The method, however,
is only applicable in the outer valence region, and is thus termed outer
valence Green´s function method (OVGF). It is discussed in detail in ref.
/29/ and /30/. The accuracy achievable is documented in ref. /31/. If
satellites of appreciable intensity accompany the main lines the ionization
energies and relative intensities have to be calculated with the so called
extended two-particle-hole Tamm-Dancoff Green´s function method (extended

2ph-TDA). This method can be used in the entire valence region. It is
also accurate to third order in the electron-electron interaction and contains
infinite selected summations such that the self energy retains the correct
analytical structure over the entire energy range. The method is extensively
discussed in the literature[32] (for earlier version of this method see
ref. [30] and [33]). The numerical aspects have been presented in ref. [34].
The Green's function calculations are based on an SCF calculation which uses
a large basis set including diffuse functions and two sets of d-type
polarization functions, namely $[12s8p2d]$ /(6s5p2d) which is derived from
a basis set by Salez and Veillard[35]. The SCF calculations were performed
with the program system MUNICH of Diercksen and Kraemer[36]. The orbital
energies are shown in table 1. The results of the OVGF and the extended 2ph-
TDA calculations are presented in table 2. The basis set has been fully
exhausted in the OVGF calculation but it had to be somewhat truncated in the
extended 2ph-TDA calculation. The two core orbitals (C1s and N1s) and their
virtual counterparts have been neglected. In addition, virtual orbitals with
an energy above 46 eV were left out in the latter calculation.

Results and Discussion

A. Energetic Considerations and Satellite Structure

We start the discussion with a comparison of the outer and inner valence
emission of NaCN at 45 eV and 1253.6 eV photon energies with the spectra
of condensed CO and N_2[7] shown in fig. 4. Note, however, that while the
NaCN 45eV spectrum was taken in an angle resolved mode in normal emission,
the spectra of condensed CO and N_2 and the 1253.6 eV spectrum of NaCN are
angle integrated[7].

For the comparison we have chosen a relative energy scale, where the
maximum of the 4σ-state[+] has been taken as reference level. This is
indicated by the dash dotted line in fig. 4. Table 3 contains the relative
binding energies of NaCN, CO and N_2.

One result is obvious: The complete valence emission of the NaCN single
crystal is determined by ion states due to ionization of the CN^- anion,
as expected. The Na2p emission is observed well below (~23 eV) the valence
band. This result supports the view that a complete charge transfer between
Na and CN moiety has taken place. Our spectra are in fair agreement with
the spectra reported by Considine et al.[20] and Vannerberg [37] who measured
HeI and HeII[20] spectra as well as monochromatized AlK_α [37] spectra respec-
tively of polycrystalline films of sodium cyanide. The relative binding
energies of the three outer valence ionizations are intermediate between
CO and N_2; however they are more similar to N_2 than to CO. In addition the

[+] The CO one-particle nomenclature is used throughout the paper for CO, N_2
and CN^-.

relative intensities of the three peaks of CN⁻ are more similar to N_2 than to
CO which is evident by inspection of fig. 4. If we excite the valence electrons
with soft x-rays, the molecular states with large atomic s-character [38] are
intensity enhanced, while those with dominating atomic p-character are
intensity suppressed. The 4σ state with large N2s character dominates the x-ray
excited spectrum, while the 1π-emission is drastically reduced. This
behaviour is in line with the observations on N_2 and CO [39]. Our assignment
of the outer valence levels is at variance with those of several other
authors [37,40] who were not able to detect the 1π emission in x-ray excited
spectra. Considine et al.[20], Vannerberg [37] and Prins and Biloen[40] report
on electron emission at energies below the three outer valence emissions of
NaCN. Vannerberg [37] reports five bands at 2.6 eV, 4.7 eV, 9.4 eV, 16.1 eV
and 23 eV relative binding energy including the Na2p emission. Prins and Biloen[40]
found three bands at :   4.7 eV, 14.2 eV and 22.4 eV below the 4σ emission.
Considine et al.[20] were only able to observe one peak about 9 eV below the
4σ band using HeII radiation.

Our results, shown in table 3, are consistent with those of Vannerberg[37].
We do not observe, however, the band at 2.6 eV relative binding energy in our
45 eV spectrum and are not able to resolve a peak in the x-ray induced spectra.
We cannot rule out ,experimentally, the possibility of a band at this energy
although our   calculations, discussed later, do not predict a satellite
with this relative binding energy(see fig. 5). The peak at 4.7 eV in the high
energy spectrum is observed as a weak feature with a photon energy of 45 eV.
Considine et al.[20] did not observe this band. In several papers, dealing with
XPS of NaCN [37,40,41] a peak between 14.5 eV and 16 eV below the 4σ level
has been reported in agreement with our results. This band is due to the emission
from the CN-σ-bond, which in a one-particle picture is termed 3σ. It is

interesting that the intensity of this state is close to zero for $h\upsilon$ = 45 eV
photon energy in the angle resolved normal emission spectrum. The strong
intensity enhancement of this band supports the high s-character of the ionized
state in agreement with our assignment to the ionization of the CN-σ-bond.

At this point it is appropriate to compare the electron emission bands
below the outer valence emissions in CN⁻ with those found in CO and N_2 [7].
In the latter cases an assignment has been extensively discussed in the
literature [5,42,43]. A simplified version [7,44] of the current assignment may
be summarized as follows: The coupling of a $\pi \rightarrow \pi^*$ excitation to a hole
state of σ symmetry, namely a configuration of type $(\sigma^{-1}\pi^{-1}\pi^*)$ leads to two
doublet states whose energy separation is determined by the singlet-triplet
splitting of the $\pi \rightarrow \pi^*$ excitation. The lowest energy $\pi \rightarrow \pi^*$ excitation in
first row diatomics is the $1\pi \rightarrow 2\pi$ excitation. If we couple this excitation
separately to the 5σ and the 4σ hole states we end up with four final states
of the type discussed above. The roman numbers I and II(Fig. 4)refer to these states
where I stands for the 5σ- and II for the 4σ-coupling. The splitting between
the components of each pair is very similar and of the order of 6 eV to 8 eV.
It is close to the singlet-triplet splitting of the $1\pi \rightarrow 2\pi$ excitation in
neutral CO and N_2 [45]. We want to point out clearly, that the above assignment
is probably oversimplified. We know from detailed calculations, that a variety
of other excited ion configurations, including two electron excitations   ,
contribute. This is particularly important for the satellites at higher relative
binding energies, close to the 3σ ionization. For the satellites at lower
binding energies, the above assignment reflects the true situation [42]. The
satellites at lower binding energy borrow their intensity from the outer
valence levels while those at higher binding energies borrow intensity from the
3σ-ionization [7].

A qualitatively similar analysis holds for CO and N_2.

The larger excitation energy for the $1\pi \rightarrow 2\pi$ excitation in N_2 as compared to CO has to be taken into account[45]. Note that the splitting of the singlet and triplet component remains basically uneffected. The energy separation between 5σ and 4σ hole states decreases for N_2. As a consequence of these two effects the satellites shift to higher relative binding energies in N_2.

If we now use the assignment for CO and N_2 as a basis to assign the inner valence electron spectrum of NaCN we end up with the dotted correlation lines shown in fig.4. As a next step to test this assignment we compare our spectrum with the result of an ext.2ph-TDA calculation on the photoelectron spectrum of the outer and inner valence electron region of CN⁻.(see ref./19/ for comparison) Fig.5 shows a direct comparison between experiment and theory. Note that the calculation was done on a free CN⁻ anion. Therefore the energy scales have been allligned for the 4σ bands. The theoretical quantity proportional to the band intensity is the so called pole strength which is equivalent to a generalized overlap amplitude and thus represents the intensity of an ionization band in sudden approximation[30,47]. We find two groups of rather intense satellites 5.5 eV and 10.8 eV below the 4σ ionization and a set of satellites in the region of 3σ ionization. The main configurations contributing to the two satellites at low relative binding energy are of type $(5\sigma^{-1}1\pi^{-1}2\pi)$ for the 5.5 eV band and $(4\sigma^{-1}1\pi^{-1}2\pi)$ for the 10.8 eV band , which is in agreement with the results of our simple considerations. For the satellites in the 3σ ionization region the situation is more complicated, as already found for CO and N_2. The coupling to various configurations leads to the broad, structured peak observed for the 3σ ionization. Still, the 3σ ionization is the most significant contribution to the peak. In comparison to CO and N_2, where the relative position of the 3σ ionization is almost identical, the CN⁻ 3σ-

ionization is found at lower binding energy. This can be rationalized on the basis of our ab-initio Hartree-Fock calculations (table I). Columns I of table 1 contain absolute energies, columns II relative energies with respect to the 4σ orbital. The latter energies are in line with the experimental observations on the 3σ ionization from fig.4 and table 3: The CN⁻-3σ-orbital is destabelized by approximately 3 eV with respect to the corresponding orbitals in CO and N_2, which are within .1 eV at the same relative energy. The reason for this effect can be found in the electronegativities of the atoms participating in the bond. Roughly, the larger the electronegativity of an atom the larger is the atomic orbital energy[48]. In the three cases, the σ-bond is formed by coupling of two atomic sp-hybride functions. In fig. 6 the situation is shown schematically for the three molecules. In CO, the oxygen function lies at high energy due to the large electronegativity of oxygen(3.5)[48]. The occupied σ- bond formed by interaction with the less electronegative carbon (2.5)[48]is situated at even higher energy. In N_2 the two interacting hybrides are degenerate and lie at intermediate energy according to the electronegativity of nitrogen (3.0)[48]. Due to the degeneracy of the interacting atomic functions the formed σ-bond is more stabelized by interaction than in the case of CO, resulting in similar relative energy. The situation for CN⁻ is equivalent to CO but due to the smaller electronegativity of nitrogen, compared to oxygen in CO, the formed σ-bond lies at lower relative energy, leading to the apparent destabelization.

Before we proceed to a discussion of absolute ionization energies a brief comment on the relative energies of the outer valence ionizations as compared with the one-particle energies shown in table 1 is appropriate. The relative binding energies of 1π and 5σ orbitals do not fit as well as those discussed for the 3σ orbital. This has to be expected since it is well known that for

N_2 a one particle description of the outer valence ionizations according to Koopmans´theorem is not appropriate[30,31]. The energy separations between the outer valence ionizations observed are not determined by relative one particle energies but rather by correlation effects[30,31]. Indeed, a comparison of orbital energies for CN⁻ in table 1 and calculated ionization potentials of table 2 reveal this effect. In the Hartree-Fock calculation with [12s/8p/2d] - basis the 1π - 5σ separation is only 0.05 eV.   However, upon inclusion of correlation effects the energy separations (table2) are almost quantitatively brought into agreement with experiment as shown in fig. 5.

The absolute binding energies of the outer valence ionizations are shown at the bottom of fig 2. The observed values are very close to what has to be expected for a completely ionic NaCN crystal:

The first ionization potential (IP) of a CN⁻ embedded in a NaCN crystal can be calculated from /49/:

$$IP = IP^{CN^-}_{free} + E_{MAD} + E_{POL} \qquad (1)$$

where $IP^{CN^-}_{free}$ is the first ionization potential of the free CN anion. This was experimentally determined by Berkowitz et al.[15] to be 3.82 eV. E_{MAD} is the Madelung energy[50] :   8.07 eV for NaCN. E_{POL} is the polarization energy according to Mott and Littleton [51]. It has been calculated for various anions in connection with ionization of alkali halides and varies between -1eV and -2eV for anions fluorine to iodine. We have assumed an intermediate value of -1.5eV. With this we calculate a first ionization potential of 10.4 eV for a completely ionic crystal which is in excellent agreement with the observed value of 10.8 eV. Note that the first ionization potential of free CN⁻ of 3.82 eV[15] is in excellent agreement with the ext. 2ph-TDA result which predicts

4.11 eV and even better when compared with the theoretical value calculated using the OVGF method[30] which is given in parentheses in table 2 (3.81 eV). Note, however, that calculated values are always vertical ionization energies.

The absolute and relative binding energies in the outer valence electron region are independent of excitation energy as revealed by fig. 2. Were the NaCN crystal a "normal" ordered solid we would observe shifts of the absolute and relative binding energies according to the sampled electron momentum of the "band-structure"[1,52]. The absence of the effect is a direct consequence of the disorder within the CN⁻ sublattice. A detailed photoemission study of absolute and relative binding energies for a NaCN phase with a rotationally ordered CN sublattice would be interesting.

The relative energies for the core ionizations are given in table 3. The absolute values can be computed referring to the first ionization energy and can be compared to binding energies of other CN containing molecules. For the solid the absolute values are: C1s =290.3 eV and N1s =405.8 eV; for the gaseous species: C1s =283.3 eV and N1s = 398.8 eV. If these values are compared with binding energies of neutral CN compounds in the gas phase: acetonitrile, C1s = 292.4 eV, N1s = 405.6 eV [53]; methylisocyanide, C1s = 292.4 eV, N1s = 406.8 eV [54]; hydrogencyanide, C1s = 293.5 eV, N1s = 406.1 eV [55], the influence of the negative charge is clearly observed. An extensive comparison of core binding energies of CN⁻ with (iso-)nitrile, (iso-)nitrilecomplexes and (iso-)nitrile-adsorbates will be given elsewhere in analogy to our studies on CO- and N_2-complexes and adsorbates[56].

B. Branching Ratios and Shape Resonances

So far we have not discussed the intensities of the outer valence electron
bands as a function of photon energy in detail. In the following we want to
compare the branching ratios of NaCN shown in fig.3 with those of gaseous
and condensed CO and N_2 reported by Plummer et al.[3] and by Fock et al.[2/+]
Note, however, that the branching ratios for CO and N_2 have been taken with
an angle integrating spectrometer, while our NaCN data were taken in an
angle resolved mode. In order to compare angle resolved and angle integrated
spectra, a possible influence of the asymmetry parameter β has to be taken
into account. Since $\beta(\omega)$ is not known for CN^-, we use the known $\beta(\omega)$ for
CO and N_2 and consider its influence of the NaCN spectra. $\beta(\omega)$ varies for the
three ion states in the outer valence electron region differently as a
function of photon energy. The extreme values are -1 and +2 [57,58] For
both CO and N_2 the smallest value is found for the 1π ionization at 20 eV
photon energy with $\beta = -.5$, the largest value for the 5σ ionization with
$\beta = 1.3$ at 40 eV photon energy [58] If we write the asymmetry-parameter
dependent cross section as:

$$\frac{d\sigma(\omega,\theta)}{d\Omega} = \frac{\sigma_{tot}}{4\pi} f(\omega) \qquad (2)$$

$$f(\omega) = \frac{\beta}{2} \left[1 + (3\cos^2\theta - 1) \right] \qquad (3)$$

where θ is the angle between the polarization vector of the light and the

---

+) The pronounced differences between the branching ratios of gasous and solid
CO and N_2 near threshold, which have been discussed in detail by Fock[2] shall
not be considered in this paper.

detection direction, then $f(\omega)$ assumes values between .9 and 1.2 for our
geometric conditions ($\theta = 45^0$). This changes the branching ratios slightly
but by no means dramatically. Particularly it does not change the habitus
of the frequency dependence of the branching ratios. We conclude that the
structure we observe in the branching ratios is not primarily caused by
the asymmetry parameter.

To assign the various features we compare our results to CO and N_2 in fig. 7[2,3]
The figure shows for each of the three outer valence ionizations the branching
ratios of gaseous and solid CO and N_2 and of CN^- in a photon energy range
between 20 eV and 40 eV. For the 5σ ionization at low photon energy we find
a dip in the branching ratio (22.5 eV) followed by a peak (25.4 eV).
A similar structure was found by Plummer et al.[3] for gaseous CO. These
authors showed that the features are not primarily the result of autoioni-
zation. They argued, that the rise in the branching ratio below the minimum
probably is a consequence of autoionization processes involving the $C^2\Sigma$-state
of CO. This state is seen in photoemission as the shake up at lowest binding
energy in fig.4. Plummer et al.[3] showed, using Davenport's[59] theoretical
results that the peak is caused by a σ- shape resonance in the continuum.
We adopt this interpretation and assign the peak at 25.4 eV photon energy to
a shape resonance of σ symmetry. The σ character of the resonance is supported
by its absence in the 1π branching ratio, which is basically independent of
photon energy except for a small, narrow peak with a maximum near the energy
of the dip in the 5σ branching ratio. The same peak in the 1π branching ratio
is found in CO and N_2 and it is not clear what causes the variations in cross
section. It is possible that interference between comparable amplitudes for
autoionization and photoionization is the reason. It is probably not connected
directly with the shape resonance, because its width is too small. The

branching ratios for the 4σ state also shows a broad resonance feature at
30 eV photon energy. The width of this structure is wider compared to the
5σ branching ratios in accord with findings for CO and N_2. The observation
of resonance structures for both σ ionizations is in agreement with the
symmetry $C_{\infty V}$ of the CN^- moiety. The intensities of the resonance structures
seem to be reduced as compared to gaseous CO and N_2. This effect has also
been observed for the 4σ resonance of CO upon condensation[2] of the gas.

In fig.3 we compare the branching ratios for the NaCN single crystal with
those taken from the work of Considine et al.[20]. Their branching ratios were
determined for a polycrystalline sample using unpolarized resonance radiation
and an angle integrating spectrometer. The HeI branching ratios agree very
well with our findings while for the HeII branching ratios our values agree
for the 1π state but differ for the 4σ and 5σ states: While for a polycrystalline
sample the branching ratios at 40 eV of 4σ and 5σ are almost identical, they
are considerably different for a single crystalline sample. We do not know what
causes the effect but we could speculate that it is due to some orientational
order within the CN^- sublattice in the NaCN single crystal. In order to shed
light on this problem one could measure the branching ratios when we sweep
through the cubic to orthorhombic phase transition at 288 K, because the CN^-
sublattice orders in the low temperature phase. However, it is not easy to
retain the single crystallinity of the sample across the phase transition.

Finally, we compare the kinetic energies of various shape resonances in CO,
N_2 and CN^- in table 4.   For com-
parison the values for adsorbed CO and N_2 are included. We find that the
kinetic energies of the CN^- shape resonances are larger than those for CO and N_2.
This is easily explained by the change in potential felt by the valence electrons

in CN^- as compared to CO and N_2. Davenport has already pointed out that a
potential change simulated in an X_α-SW calculation by altering the α-parameter
leads to changes in the position of the shape resonance[59]. A change of the
potential also occurs upon adsorption of a molecule[61]. This leads to a
drastic shift of the shape resonance and to a decrease of its width.
Calculations using small CO-metal clusters reproduce this effect quantitatively[62].
Very recently, Schichl et al[62] presented a rather detailed study of these
effects. Greuter et al.[4], earlier used qualitative arguments and arrived at
similar-not as detailed- conclusions. Both groups of authors conclude that
chemisorption changes the wave functions of the molecule and   may partly
cause the observed changes of the shape resonance. The present data on CN^-
add more evidence to this picture. As stated in the introduction, the electron
distribution in CN^- is different from CO and N_2. Therefore we can take CN^- as
a model to study how wavefunction changes influence the position of the
shape resonance. Table 4   shows that a wavefunction change does
influence the position of the shape resonance. The effect is of the order of
30 % to 60 % of the shift induced by chemisorption. The missing portion of
the shift is possibly due to the influence of the substrate in the final
state.

Summary and Conclusion

We have presented angle resolved photoelectron spectra of a NaCN (001) single
crystal surface. Synchrotron UV radiation and conventional x-ray tube radiation
induced electron distribution curves show that the valence ionization spectra
between 10 eV and 40 eV binding energy are exclusively determined by emission
from the CN⁻ sublattice. The first Na emission (Na2p) appears 23 eV below
the 4σ emission. The latter result, together with the measured absolute
binding energies support the view that the outer sodium electron has been
completely transferred towards the CN moieties which form the CN⁻ sublattice.
Photon energy dependent spectra show no variation of absolute and relative
binding energies of the CN⁻ ionizations. This is in agreement with results
from neutron diffraction studies[16] showing that the CN⁻ anions rotate on their
lattice positions and thus form a "coulomb stabelized" CN⁻ gas.

The satellite structure, observed in the inner valence electron region can
be interpreted on the basis of a comparison to condensed CO and N_2 and to
many-body corrected calculations on the CN⁻ anion reported in this paper.

The branching ratios of the outer valence levels show resonance structures
in both σ levels, but not in the π level in agreement with the $C_{\infty v}$ symmetry
of the CN⁻ moiety. The position of the shape resonances in CN⁻ are different
from CO and N_2. It is argued that this is due to a potential change in CN⁻.
The observed shifts of the CN⁻ shape resonances are between 30% to 60% of the
shifts found when CO or N_2 are adsorbed on transition metal surfaces. We
suggest that the shift observed in CN⁻ is basically due to the different
electron distribution in CN⁻ as compared to CO and N_2 and that the remaining
contribution of 70% to 40% to the shift found upon chemisorption is due to
the influence of the metal substrate on the final state observed in photo-
ionization.

References

/1/   E.W. Plummer, W. Eberhardt; Adv. Chem. Phys. 49, 533 (1982)

/2/   J.-H. Fock, H.J. Lau, E.E. Koch; Chem. Phys. 83, 377 (1984);

      H.-J. Lau, J.-H. Fock, E.E. Koch; Chem. Phys. Letters 89, 281 (1982);

      J.-H. Fock; Thesis, Hamburg (1983) unpublished

/3/   E.W. Plummer, T. Gustafsson, W. Gudat, D.E. Eastman; Phys. Rev. A15,

      2339 (1977)

/4/   F. Greuter, D. Heskett, E.W. Plummer, H.-J. Freund;

      Phys. Rev. B27, 7117 (1983)

/5/   J. Schirmer, L.S. Cederbaum, W. Domcke, W. von Niessen; Chem. Phys. 26, 149 (1977)

/6/   S. Krummacher, V. Schmidt, F. Wuilleumier; J. Phys. B: 13, 3993 (1980); S. Krummacher,

      V. Schmidt, F. Wuilleumier, J.M. Bizau, D. Ederer; J. Phys. B: 16, 1733 (1983)

/7/   W. Eberhardt, H.-J. Freund; J. Chem. Phys. 78, 700 (1983)

/8/   R. Bonaccorsi, C. Petrongolo, E. Scrocco, J. Tomasi;

      J. Chem. Phys. 48, 1500 (1968)

/9/   E. Clementi, D. Klint; J. Chem. Phys. 50, 4899 (1969)

/10/ J.B. Moffat, H.E. Popkie; J. Mol. Struct. 6, 155 (1970)

/11/ K.M. Griffing, J. Simons; J. Chem. Phys. 64, 3610 (1976)

/12/ P.R. Taylor, G.B. Bacskay, N.S. Hush, A.C. Hurley;

      J. Chem. Phys. 70, 448 (1979)

/13/ G. Natta, L. Passerini; Gazz. Chim. Ital. 61, 191 (1931)

/14/ H.J. Verweel, J.M. Bijvoet; Z. Krist. 100, 8201 (1938)

/15/ J. Berkowitz, W.A. Chupka, T.A. Walter; J. Chem. Phys. 50, 1497 (1969)

/16/ J.M. Rowe, D.G. Hinks, D.L. Price, S. Susman, J.J. Rush;

      J. Chem. Phys. 58, 2039 (1973)

/17/ J.M. Bijvoet, J.A. Lely; Rec. Trav. Chem. Pays-Bas 59, 908 (1940)

/18/ see for example:

      a) S. Haussühl; Sol. State Comm. 13, 147 (1973); b) K. Strässner,

      W. Henkel, H.D. Hochheimer, M. Cardona; Sol. State Comm. 47, 567 (1983);

      c) C.H. Wang, S.K. Satija; J. Chem. Phys. 67, 851 (1977)

/19/ W. von Niessen, R. Cambi; " The effect of the substituent in the

      Cyanide Series, ClCN, BrCN, NaCN and KCN: A Green's Function

      Approach to the Valence Ionization Spectra"; J. Electr. Spectr. in press

/20/ M. Considine, J.A. Connor, I.H. Hillier; Inorg. Chem. 16, 1392 (1977)

/21/ R. Engelhardt; Diploma Thesis, Hamburg (1982) unpublished,

      C.A. Feldmann, R. Engelhardt, T. Premien, E.E. Koch, V. Saile;

      Nucl. Instr. Methods 208, 785 (1983)

/22/ H.D. Polaschegg; Appl. Phys. 4, 63 (1974)

/23/ R.A. Pollak, S.P. Kowalczyk, L. Ley, D.A. Shirley; Phys. Rev. Letters

      29, 274 (1972): 4d(17.64 eV/16.74 eV)

/24/ B. Marquardt; unpublished

/25/ S.F. Boys; Proc. Roy Soc. (London) A200, 542 (1950)

/26/ S. Huzinaga; Prog. Theor. Phys. (Suppl) 40, 52 (1967)

/27/ W.J. Hehre, F. Stewart, J.A. Pople; J. Chem. Phys. 51, 2657 (1969)

/28/ J.S. Binkley, J.A. Pople, W.J. Hehre; J. Amer. Chem. Soc. 102, 939 (1980)

/29/ L.S. Cederbaum; Theor. Chim. Acta 31, 239 (1973); J. Phys. B 8, 290 (1975)

/30/ L.S. Cederbaum, W. Domcke; Adv. Chem. Phys. 36, 205 (1977)

/31/ W. von Niessen, G.H.F. Diercksen, L.S. Cederbaum; J. Chem. Phys. 67,

      4124 (1977)

/32/ J. Schirmer, L.S. Cederbaum, O. Walter; Phys. Rev. A28, 1237 (1983)

/33/ J. Schirmer, L.S. Cederbaum; J. Phys. B11 1889 (1978)

/34/ W. von Niessen, J. Schirmer, L.S. Cederbaum; Comp. Phys. Reports 1,

      57 (1984)

/35/ C. Salez, A. Veillard; Theor. Chim. Acta 11, 441 (1968)

/36/ G.H.F. Diercksen, W.P. Kraemer; MUNICH: Molecular Program System

      Reference Manual, Special Technical Report, Max-Planck-Institut für

      Physik und Astrophysik, Munich, to be published;

      G.H.F. Diercksen; Theor. Chim. Acta 33, 1 (1974)

/37/ N.-G. Vannerberg; Chem. Scripta 9, 122 (1976)

/38/ U. Gelius in " Electron Spectroscopy" (Ed. D.A. Shirley), North-Holland
Publishing Comp., Amsterdam (1971)

/39/ K. Siegbahn et al. " ESCA-Applied to Free Molecules", North-Holland
Publ. Comp., Amsterdam (1971)

/40/ R. Prins, P. Biloen; Chem. Phys. Letters 30, 340 (1975)

/41/ W.H. Morrison, D.N. Hendrickson; Inorg. Chem. 11, 2600 (1972)

/42/ J. Schirmer, O. Walter; Chem.Phys. 78, 201 (1983)

/43/ P.W. Langhoff, S.R. Lang hoff, T.N. Resigno, J. Schirmer,
L.S. Cederbaum, W. Domcke, W. von Niessen; Chem.Phys. 58, 71 (1981)

/44/ G. Wendin in " Structure and Bonding" Vol. 45, Springer Verlag, Berlin
(1981)

/45/ E.N. Lassettre; Can. J. Chem. 47, 1733 (1969)

/46/ P.S. Bagus, E.K. Viinikka; Phys. Rev. A15, 1486 (1977)

/47/ T. Åberg; Ann. Acad. Sci. Fenn. Ser. A6: 308, 1 (1969)

/48/ L. Pauling; "The nature of the Chemical Bond and the Structure of
Molecules and Crystals" Cornell University Press (1960)

/49/ J. Berkowitz; in "The Alkali Halide Vapors" (Eds. P. Davidovits, D.L.
McFadden) Academic Press, New York (1979)

/50/ M. Born, J.E. Mayer; Z. Phys. 75, 1 (1932)

/51/ N. F. Mott, M.J. Littleton; Trans. Farad. Soc. 34, 485 (1938)

/52/ F. J. Himpsel; Appl. Opt. 19, 3964 (1980)

/53/ W.L. Jolly, T.F. Schaaf unpublished data, and A.A. Bakke, H.-W. Chen,
W.L. Jolly; J. Electr. Spectr. Rel. Phen. 20, 333 (1980)

/54/ P. Brant; J. Electr. Spectr. Rel. Phen. 33, 153 (1984)

/55/ T.D. Thomas; R.W. ShawJr.; J. Electr. Spectr. Rel. Phen. 5, 108 (1974)

/56/ H.-J. Freund; Habilitationsschrift, Köln (1983) unpublished

/57/ J.C. Tully, R.S. Berry, B.J. Dalton; Phys. Rev. 176, 95 (1968)

/58/ W. Thiel; Chem. Phys. 77, 103 (1983) and references therein

/59/ J.W. Davenport; Phys. Rev. Letters 36, 945 (1976) and J. W. Davenport;
Thesis, University of Pennsylvania (1976) unpublished

/60/ C.L. Allyn, T. Gustafsson, E.W. Plummer; Chem. Phys. Letters 47, 127 (1977)

/61/ J.W. Davenport; J. Vac. Sci. Technol. 15, 433 (1978)

/62/ A. Schichl, D. Menzel, N. Rösch; Chem. Phys. 105, 285 (1984)

/63/ K. Horn, J. DiNardo, W. Eberhardt, H.-J. Freund, E.W. Plummer;
Surf. Sci. 118, 465 (1982)

/64/ H.-J. Lau; Diploma Thesis, University Hamburg (1982), unpublished,
Internal Report HASYLAB 82-01, March 1982

- 25 -

Captions to Tables

Table 1   Hartree-Fock orbital energies for CO, N$_2$ and CN$^-$(in eV) using
a 3-21G Basis. Column I contains the absolute, column II the
relative orbital energies (see text). For each molecule the
total energy is given at the bottom.
The valence electron orbital energies of CN$^-$ calculated with
a 12s/8p/2d basis are shown in addition.

Table 2   Results of the extended 2ph-TDA calculation on CN$^-$ using the
[12s/8p/2d] -basis set. The calculated ionization potentials
(IP) given in parentheses have been calculated using the OVGF
method[30]. Pole strengths (PS) are given for the extended
2ph-TDA results. The hole states given in parentheses are those
to which the given excited configurations couple.
[a]) σ^*,π^* denote virtual orbitals of these symmetries. Because
the basis set contains Rydberg functions they are in general
not the lowest virtual orbitals of this symmetry. It is
however obvious from the calculation that excitations into
Rydberg type orbitals also do contribute although they are
not dominant.

Table 3   Experimental ionization energies for CO, N$_2$ and NaCN relative
to the position of the 4 σ state. Negative values refer to lower,
positive values to higher relative binding energies. [a]) ref./39/

Table 4   Kinetic energies of shape resonances for the σ levels of various
systems in eV. The CO nomenclature is used throughout.

Table 1

Sym	CO I E_{orb}(eV)	CO II E_{rel}(eV)	N$_2$ I E_{orb}(eV)	N$_2$ II E_{rel}(eV)	CN$^-$ I E_{orb}(eV)	CN$^-$ II E_{rel}(eV)	CN$^-$ E_{orb}(eV) (12s/8p/2d)
1σ	-559.747	538.385	-424.601	403.872	-411.774	404.260	-
2σ	-307.841	286.479	-424.576	403.847	-294.689	287.175	-
3σ	-42.841	20.734	-41.317	20.729	-24.381	16.867	-25.322
4σ	-21.362	0.0	-20.588	0.0	-7.514	0.0	-9.249
1π	-17.266	-4.095	-16.853	-3.735	-3.933	-3.581	-9.302
5σ	-14.777	-6.585	-16.762	-3.826	-3.531	-3.983	-5.251
2π	4.397	-	5.058	-	15.096	-	-
6σ	13.388	-	20.720	-	23.051	-	-
E$_{tot}$	-134.591064 a.u.		-132.243149 a.u.		-110.909348 a.u.		

CN⁻ [12s/8p/2d]

Sym	IP	PS	Hole	2ph-excitation [a]
States of σ symmetry	4.11 (3.81)	0.87	5σ	
	7.55	0.81	4σ	
	13.01	0.053	(4σ)	$5\sigma^{-1}1\pi^{-1}\pi^{*}$
	17.80	0.068	(3σ)	$5\sigma^{-1}1\pi^{-1}\pi^{*}$, $5\sigma^{-2}\sigma^{*}$
	18.46	0.059	(3σ)	$4\sigma^{-1}1\pi^{-1}\pi^{*}$, ...
	18.88	0.009	(3σ)	
	22.72	0.074	(3σ)	$5\sigma^{-1}1\pi^{-1}\pi^{*}$, $4\sigma^{-1}1\pi^{-1}\pi^{*}$
	23.31	0.150	(3σ)	$4\sigma^{-1}5\sigma^{-1}\sigma^{*}$, $5\sigma^{-2}\sigma^{*}$, $4\sigma^{-2}\sigma^{*}$, $1\pi^{-2}\pi^{*}$
States of π symmetry	5.60 (5.11)	0.88	1π	
	17.68	0.008	(1π)	$1\pi^{-1}5\sigma^{-1}\sigma^{*}$

Table 2

State	CO	NaCN	N₂
5σ	-5.98	-3.33	-2.93
1π	-2.79	-2.0	-1.46
4σ	0.0	0.0	0.0
	2.93	4.66	6.52
	5.59	8.91	10.77
	8.25	10.91	13.03
	12.24	14.90	18.75
3σ	19.29	16.23	19.42
Na2p		23.14	
C1s	275.8 [a]	276.10	
N1s		391.64	391.3 [a]
O1s	522.0 [a]		

Table 3

system	5 σ	4 σ	ref.
CO gas	9.6	12.3	/3/
CO solid	9.8	14.7	/64/
N$_2$ gas	12.5	-	/3/
N$_2$ solid	12.9	-	/2/
CN$^-$	14.1	14.6	
CO/Ni(100)	16.8	18.2	/60/
CO/Co(0001)	16.9	16.0	/4/
CO/Co(0001) high coverage	18.2	18.5	/4/
N$_2$/Ni(110)	15.0	14.5	/63/

Table 4

Figure 1   a) Schematic representation of the crystal structure of the
cubic phase of NaCN. Only the first two layers of a (100)-
surface are shown. /13/

b) Angular dependence of the density of C and N atoms on a sphere
of radius one half of the CN bond length. The cube indicates
the varous directions within the crystal./16/

Figure 2   Set of angle resolved photoelectron spectra taken with
synchrotron radiation for different excitation energies. The
geometry of the experiment is indicated. The absolute binding
energies of the three outer valence electron levels are given
at the bottom (in eV).

Figure 3   Branching ratios for the three outer valence levels between 20 eV
and 45 eV photon energy.

Figure 4   Comparison of the valence photoelectron spectra of NaCN taken with
45 eV (normal emission) and 1253.6 eV (angle integrated) photon
energies with those of condensed CO and N$_2$ /7/. The spectra have
been alligned at the maximum of the 4σ emission.

Figure 5   Comparison of the experimental valence photoelectron spectrum of NaCN
with a many-body corrected Hartree-Fock calculation on the CN$^-$ anion.
The calculated 4σ ionization energy has been alligned with the ex-
perimental 4σ ionization energy.

Figure 6   Schematic representation of the interaction of two atomic sp-hybride
functions to form a σ bond in CO, N$_2$ and CN$^-$.

Figure 7   Comparison of experimental branching ratios of gaseous[3] and
solid[2] CO and N_2 with CN^- between 20 eV and 45 eV photon
energy. a) 5σ ionization, b) 1π ionization, c) 4σ ionization.
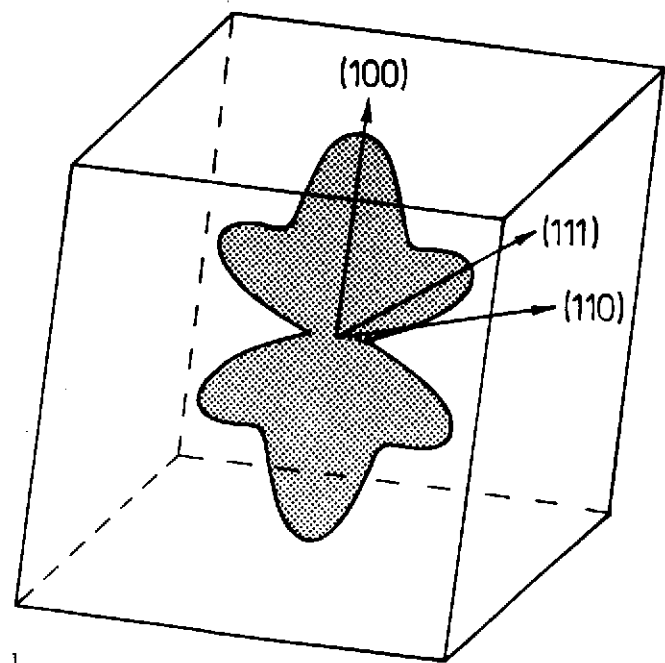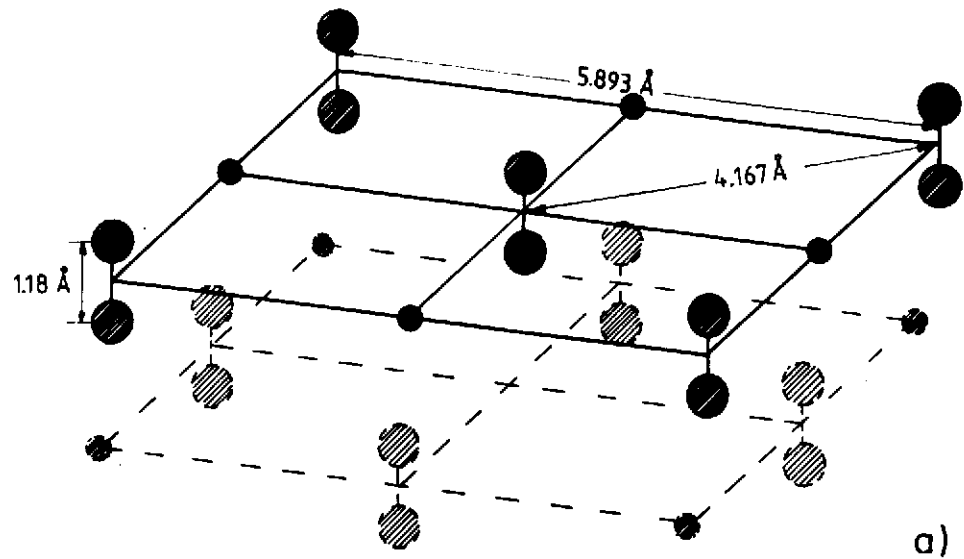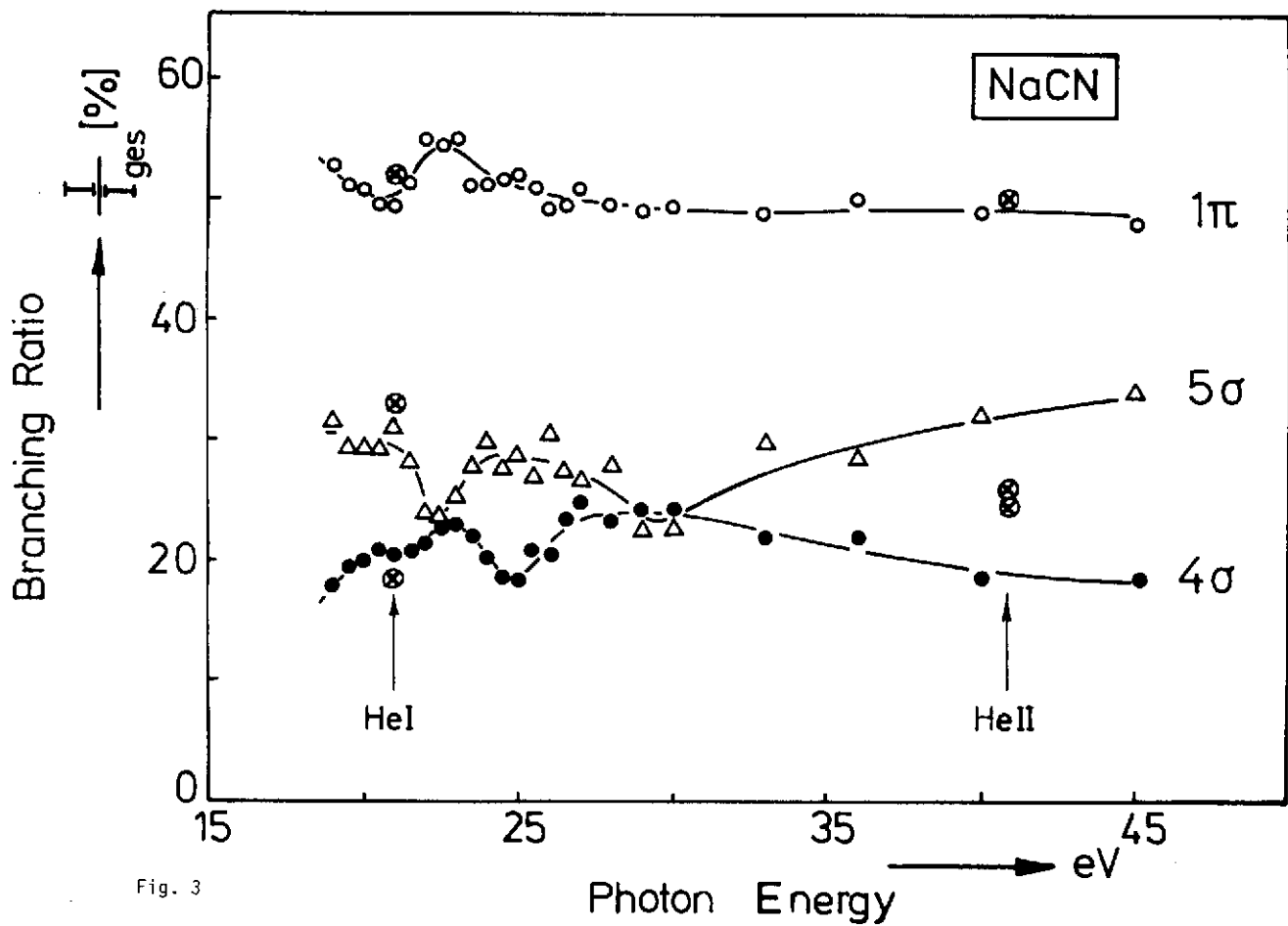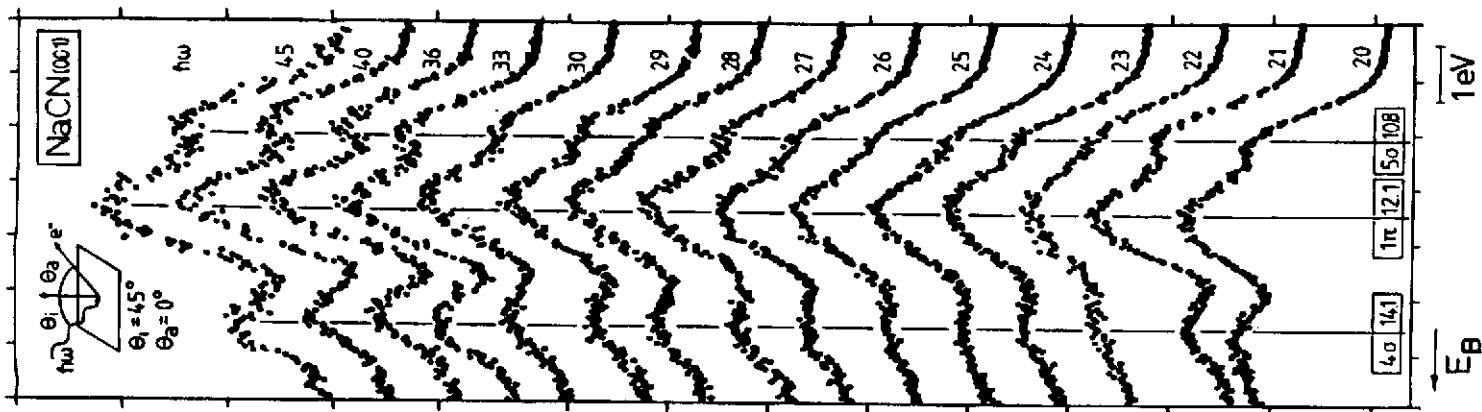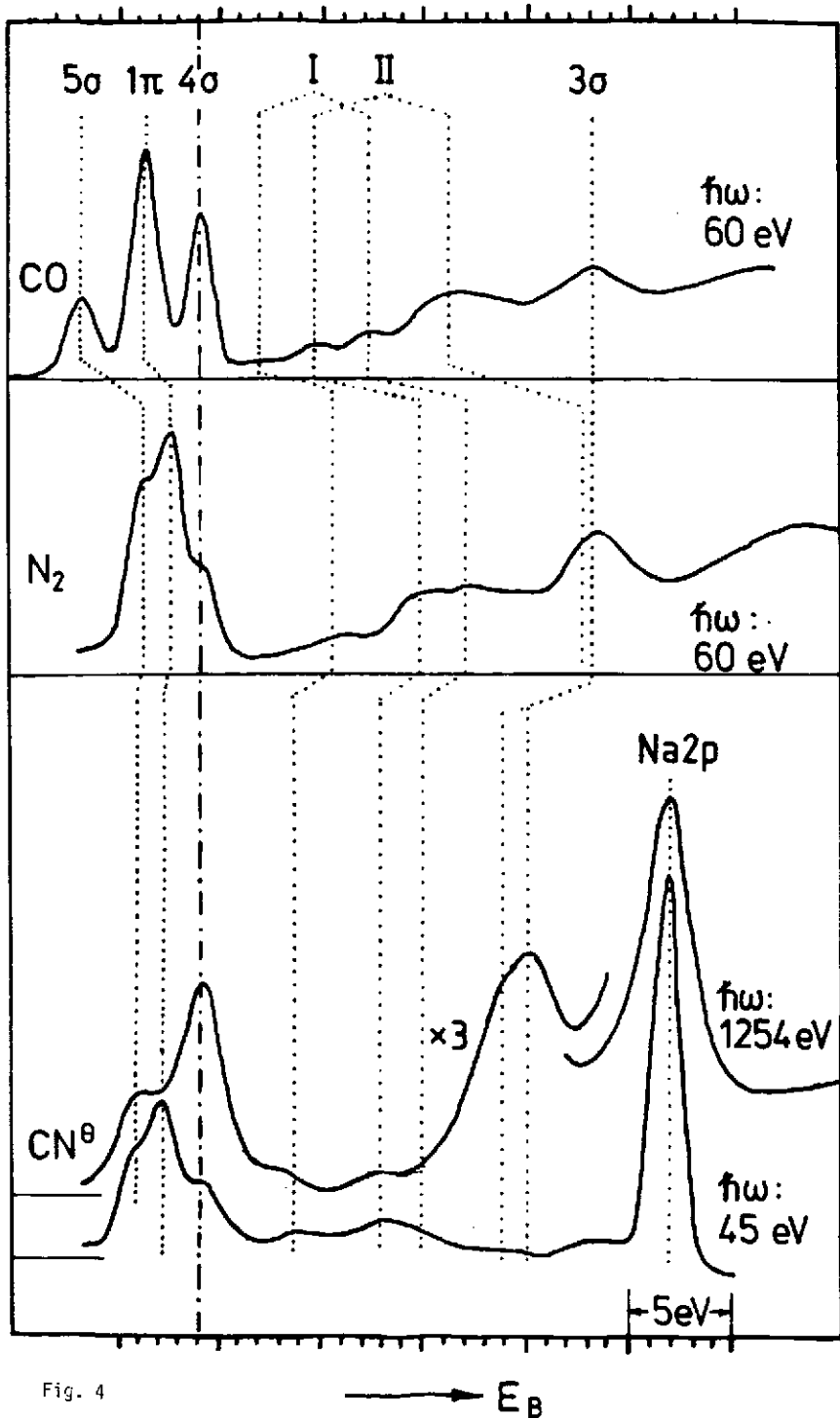The abszissa is identical for all systems.

5.893 Å

4.167 Å

1.18 Å

a)

(100)

(111)

(110)

b)

Fig. 1

Fig. 3

Fig. 2

Fig. 4

Fig. 5

CO

5σ 1π 4σ I   II 3σ

$\hbar\omega$: 60 eV

N_2

$\hbar\omega$: 60 eV

$CN^{\ominus}$

Na2p

×3

$\hbar\omega$: 1254 eV

$\hbar\omega$: 45 eV

├─5eV─┤

E_B

NaCN (001) EXPERIMENT

Na2p

$\hbar\omega$: 1253.6eV

$\hbar\omega$: 45eV

$CN^{\ominus}$ THEORY

1π

5σ

4σ

$5\bar{\sigma}\,1\bar{\pi}\,\pi^*$

$4\bar{\sigma}\,1\bar{\pi}\,\pi^*$

3σ

├─5eV─┤

Binding Energy ──→ (eV)

Fig. 7

Fig. 6